Original Article

TIMP-1 Promotes Expression of MCP-1 and Macrophage Migration by Inducing Fli-1 in Experimental Liver Fibrosis

Xiaoli Huang[1,2#], Xiaofan Wang[1,2#], Yanhong Wang[1,2,3#], Shuangjun Shen[1,2], Wei Chen[4], Tianhui Liu[1,2], Ping Wang[1,2], Xu Fan[1,2], Lin Liu[1,2], Jidong Jia[1,2] and Min Cong[1,2*]

[1]*Liver Research Center, Beijing Friendship Hospital, Capital Medical University, Beijing, China;* [2]*Beijing Key Laboratory of Translational Medicine in Liver Cirrhosis and National Clinical Research Center of Digestive Disease, Beijing, China;* [3]*Dongying People's Hospital, Dongying, Shandong, China;* [4]*Experimental and Translational Research Center, Beijing Friendship Hospital, Capital Medical University, Beijing, China*

Abstract

Background and Aims: Tissue inhibitor of metalloproteinase-1 (TIMP-1) plays a role in the excessive generation of extracellular matrix in liver fibrosis. This study aimed to explore the pathways through which TIMP-1 controls monocyte chemoattractant protein-1 (MCP-1) expression and promotes hepatic macrophage recruitment. ***Methods:*** Liver fibrosis was triggered through carbon tetrachloride, and an adeno-associated virus containing small interfering RNA targeting TIMP-1 (siRNA-TIMP-1) was administered to both rats and mice. We assessed the extent of fibrosis and macrophage recruitment. The molecular mechanisms regulating macrophage recruitment by TIMP-1 were investigated through transwell migration assays, luciferase reporter assays, the use of pharmacological modulators, and an analysis of extracellular vesicles (EVs). ***Results:*** siRNA-TIMP-1 alleviated carbon tetrachloride-induced liver fibrosis, reducing macrophage migration and MCP-1 expression. Co-culturing macrophages with hepatic stellate cells (HSCs) post-TIMP-1 downregulation inhibited macrophage migration. In siRNA-TIMP-1-treated HSCs, microRNA-145 (miRNA-145) expression increased, while the expression of Friend leukemia virus integration-1 (Fli-1) and MCP-1 was inhibited. Downregulation of Fli-1 led to decreased MCP-1 expression, whereas Fli-1 overexpression increased MCP-1 expression within HSCs. Transfection with miRNA-145 mimics reduced the expression of both Fli-1 and MCP-1, while miRNA-145 inhibitors elevated the expression of both Fli-1 and MCP-1 in HSCs. miRNA-145 bound directly to the 3'-UTR of Fli-1, and miRNA-145-enriched EVs secreted by HSCs after TIMP-1 downregulation influenced macrophage recruitment. ***Conclusions:*** TIMP-1 induces Fli-1 expression through miRNA-145, subsequently increasing MCP-1 expression and macrophage recruitment. MiRNA-145-enriched EVs from HSCs can transmit biological information and magnify the function of TIMP-1.

Citation of this article: Huang X, Wang X, Wang Y, Shen S, Chen W, Liu T, *et al*. TIMP-1 Promotes Expression of MCP-1 and Macrophage Migration by Inducing Fli-1 in Experimental Liver Fibrosis. J Clin Transl Hepatol 2024;12(7):634–645. doi: 10.14218/JCTH.2023.00514.

Introduction

Chronic liver disease has emerged as a global health challenge, contributing to approximately 2 million fatalities annually worldwide.[1,2] Liver fibrosis, a critical manifestation of chronic liver disease caused by factors such as viral hepatitis, alcohol abuse, and metabolic syndromes, can progress to cirrhosis and hepatocellular carcinoma if left unaddressed.[3,4] The progression of liver fibrosis is characterized by an imbalance in extracellular matrix (ECM) synthesis and degradation, signifying a pivotal shift in liver homeostasis toward excessive ECM accumulation. Matrix metalloproteinases (MMPs) and their natural inhibitors, tissue inhibitors of metalloproteinases (TIMPs), are central to the regulation of ECM remodeling, with TIMP-1 emerging as a key factor in the fibrotic process.[5] The activation of hepatic stellate cells (HSCs) to ECM-secreting myofibroblasts, a hallmark of liver fibrogenesis, is accompanied by TIMP-1 upregulation.[6] This upregulation inhibits MMP activity, prevents ECM degradation, and supports HSC survival, thereby promoting fibrosis.[7,8]

We previously generated a recombinant adeno-associated virus (rAAV) harboring siRNA targeting the TIMP-1 gene (rAAV/siRNA-TIMP-1) and examined its impact on liver fibrosis in rats. The administration of rAAV/siRNA-TIMP-1 significantly inhibited TIMP-1 expression in HSCs, mitigating liver fibrosis induced by both carbon tetrachloride and bile duct ligation. Furthermore, the treatment resulted in a reduction in the expression of α-smooth muscle actin (α-SMA) and transforming growth factor-β (TGF-β).[9] TGF-β, a pro-fibrotic mediator primarily released by recruited macrophages during chronic liver injury, triggers HSC activation and promotes ECM production. It has been reported that monocyte chemoattractant protein (MCP)-1 stimulates the recruitment of monocyte-derived macrophages that activate myofibroblasts.[10] Our previous research indicated that the suppression of TIMP-1 expression in rat liver fibrosis might be associated with a reduction in

the recruitment of macrophages to the damaged liver. This observation has led us to delve deeper into the mechanisms by which TIMP-1 affects macrophage recruitment, specifically through MCP-1 expression regulation.

Several studies have demonstrated the diverse functions of TIMP-1, attributing them to its interactions with micro-RNAs.[11,12] In experimental atherosclerosis, the vascular smooth muscle cell-specific augmentation of miRNA-145 mitigates atherosclerosis, enhances plaque stability, and reduces plaque inflammation. This is evident from a decline in macrophage infiltration and serum MCP-1 levels.[13] Furthermore, the Friend leukemia virus integration (Fli)-1 transcription factor stimulates the transcription of MCP-1 directly by binding to the promoter and indirectly by interacting with other transcription factors.[14] Additionally, miRNA-145 has been identified as a regulator of Fli-1.[13,15] In this study, we aimed to delve deeper into the molecular mechanisms governing the role of TIMP-1 in regulating MCP-1 via miRNA-145, utilizing rodent models for both *in vivo* and *in vitro* analyses. We also clarified the pathways through which TIMP-1 influences MCP-1 regulation by miRNA-145, including the involvement of its direct target gene, *Fli-1*, in primary HSCs.

Extracellular vesicles (EVs) are cell-derived vesicles, ranging from 40 to 160 nm in diameter, found in various eukaryotic fluids. They are formed by the segregation of intracellular polyvesicles with cell membranes and are subsequently released into the extracellular space. After release, EVs adhere to recipient cells, conveying biologically active molecules such as proteins, miRNA, mRNA, and DNA. Subsequently, the recipient cells may undergo epigenetic reprogramming and consequent phenotypic changes based on the biomolecular information they receive.[16,17] In this study, we investigated the expression levels of miRNA-145 in the EVs released by HSCs following the downregulation of TIMP-1 expression. Additionally, we sought to determine whether these EVs possess the capability to augment the effects of TIMP-1.

Methods

Development and assembly of rAAV/siRNA-TIMP-1 and rAAV/EGFP

The rAAV/siRNA-TIMP-1 and rAAV/enhanced green fluorescent protein (EGFP) constructions were generated following previously outlined methods.[9] Subsequently, Cyagen Biosciences Inc. (Guangzhou, China) packaged rAAV/siRNA-TIMP-1 and rAAV/EGFP at concentrations of 1×10^{12} and 2×10^{12} vector genomes per milliliter (v/v) upon purification, respectively.

Animal models

Male C57BL/6 mice (18–22 g) and Wistar rats (180–220 g) were purchased from Beijing Vital River Laboratory Animal Technology Co., Ltd. (Beijing, China). The animals were exposed to a 12:12-h light/dark cycle in a regulated temperature environment and were provided unrestricted access to standard chow and sterile water. All procedures related to the care and experimentation involving animals adhered to the regulations outlined in the guidelines for the use of laboratory animals established by the Beijing Friendship Hospital, Capital Medical University (Protocol Number:18-2001).

The mice and rats were randomly allocated into four groups: control, CCl_4, CCl_4 + rAAV/EGFP, and CCl_4 + rAAV/siRNA-TIMP-1. In the CCl_4 group, male C57BL/6 mice received intragastric administration (i.g.) of 20% CCl_4 dissolved in olive oil (1:4, v/v) at a dosage of 10 μL/ g body weight twice weekly for 6 weeks.[18] Similarly, male Wistar rats were intraperitoneally (i.p.) injected with 40% CCl_4 dissolved in olive oil (4:6, v/v) at a dosage of 200 μL/100g body weight twice weekly for four weeks.[9] In the CCl_4 + rAAV/EGFP and CCl_4 + rAAV/siRNA-TIMP-1 groups, on the day following the initial CCl_4 injection, mice received saline injections containing 1×10^{10} v.g. of the respective recombinant viruses via the tail vein, whereas rats were injected with saline containing 4×10^{10} v.g. of the respective recombinant viruses via the tail vein. The corresponding doses of olive oil were injected i.p. or i.g. as a control. After CCl_4 treatment for six weeks (for mice) or four weeks (for rats), the animals were sacrificed under sodium pentobarbital anesthesia for further analysis.

Histological examination

Liver specimens were fixed in 4% paraformaldehyde, embedded in paraffin, and sectioned. Staining procedures included hematoxylin and eosin (H&E) staining, Masson staining, and immunohistochemistry staining for ED-1 (Abcam, Cambridge, UK) and F4/80 (Abcam, Cambridge, UK).[19]

Cell culture

Primary HSCs were isolated from C57BL/6 mice following a previously outlined protocol with some adjustments.[20,21] Briefly, mice primary HSCs were isolated by a two-step collagenase perfusion and obtained by density gradient centrifugation. The culture medium for primary HSCs comprised DMEM (Hyclone, Utah, USA), Ham's F12K (Gibco, Grand Island, NY, USA), 15% fetal bovine serum (FBS; Gibco, Grand Island, NY, USA), and 1% penicillin/streptomycin (Solarbio, Beijing, China). The rat HSC-T6 line, provided by Prof. Friedman (Mount Sinai Hospital, NY, USA), was used. Mouse macrophage line RAW264.7 and rat macrophage line CRL-2192 cells were acquired from the Cell Resource Center of the Institute of Basic Medical Sciences of the Chinese Academy of Medical Sciences. The culture medium for HSC-T6, CRL-2192, and RAW264.7 comprised DMEM and 10% FBS.

Immunofluorescence

Immunofluorescence was performed as previously described.[22] Primary HSCs underwent fixation, permeabilization, and blocking, followed by overnight incubation with either mouse anti-α-SMA antibody (Abcam, Cambridge, UK) or rabbit anti-desmin antibody (Abcam, Cambridge, UK). This was followed by washing and incubation with donkey anti-mouse Alexa Fluor 488 (Invitrogen, Carlsbad, CA) or donkey anti-rabbit Alexa Fluor 594 (Invitrogen, Carlsbad, CA). Nuclei were counterstained using 4',6-diamidino-2-phenylindole (DAPI; Beyotime, Shanghai, China). Observation and photography of cells were conducted using fluorescent microscopy.

Transfection

HSCs were transfected using Lipofectamine 2000 reagent (Invitrogen, Carlsbad, CA, USA) for 48 h with siRNA negative control (NC), siRNA-TIMP-1, siRNA-Fli-1, Fli-1 overexpression plasmid, miRNA-145 mimics NC, miRNA-145 mimics, miRNA-145 inhibitor NC, and miRNA-145 inhibitor.[23,24] Subsequently, the cells were collected for further experiments. The sequences of siRNAs and miRNA modulators used are listed in Supplementary Table 1.

Transwell migration assay

Macrophage migration was assessed utilizing a Corning 8.0 μm Transwell cell culture chamber (Corning, NY, USA). HSCs were transfected with TIMP-1 siRNA or NC. After 6 h, the transfection mixture was replaced with fresh medium. Macrophages (RAW 264.7 cells or CRL-2192 cells) were then introduced into the upper chamber. After 48 h of co-culture, non-mi-

gratory macrophages were cleared from the upper chamber with a cotton swab, and the cells on the lower surfaces were fixed with 4% paraformaldehyde as previously described.[25] Macrophages were stained with DAPI and counted under a microscope in five randomly selected high-power fields.

Luciferase reporter assays

Bioinformatic analysis identified two possible miRNA-145 binding sites in the Fli-1 3'-UTR. The 3'-UTR fragments from the wild-type Fli-1 were amplified and inserted into the NheI-HindIII site of the pGL4 control vector. To generate the mutated Fli-1 3'-UTR vector, the eight nucleotides AACTGGAT and/or AACTGGAA were replaced with GGTGATCG in the reporter construct. The luciferase reporter construct (Fli-1 3'-UTR) was co-transfected with miRNA-145 mimics or control into 293 cells using Lipofectamine 2000 (Invitrogen, Carlsbad, CA) for 48 h. Relative luciferase activity was measured using a dual-luciferase reporter assay system (Promega, Madison, WI, USA).[26]

Extracellular vesicle isolation, characterization, and uptake

Extracellular vesicle isolation was carried out following a previous protocol with some adjustments.[27] The supernatants from the cell culture were collected and centrifuged at 2,500 g for 30 m, and then at 10,000 g for 30 m to remove cells and debris. Subsequently, the resulting supernatants were ultracentrifuged twice at 110,000 g for 70 m. The EVs were resuspended in PBS and preserved at −80°C. To examine the EVs, a 10 µL sample of the enriched solution was deposited on a copper mesh, treated with 2% uranyl acetate for contrast, and imaged using a transmission electron microscope (JEOL-JEM1400, Tokyo, Japan). The size and quantity of the isolated particles were determined using a ZetaView PMX 110 (Particle Metrix, Meerbusch, Germany) equipped with a 405 nm laser. Videos of 60 seconds, recorded at a rate of 30 frames per second, were analyzed for particle movement using nanoparticle tracking analysis (NTA) software (ZetaView 8.02.28). The characterization of EVs was conducted through western blot analysis employing antibodies targeting the EV markers cluster of differentiation (CD) 9 (Abcam, Cambridge, UK), CD63 (Abcam, Cambridge, UK), and tumor-susceptibility gene (TSG) 101 (Abcam, Cambridge, UK).

To assess the uptake of EVs by HSCs and macrophages, EVs obtained from primary HSCs were labeled with PKH26 (Sigma-Aldrich, St. Louis, MO, USA). PKH26-labeled EVs were added to HSCs and macrophages separately and incubated for 24 h.

miRNA high-throughput sequencing

Total RNA from EVs was purified using the miRNeasy® Mini kit (QIAGEN, Frederick, MD, USA). The RNA concentration, purity, and integrity were evaluated using Qubit 2.0 (Life Technologies, USA), Nanodrop (Thermo Fisher Scientific, Rockford, IL, USA), and Agilent 2100 bioanalyzer (Agilent Technologies, USA), respectively. For small RNA sequencing library generation, one microgram of RNA was utilized with the QIAseq miRNA Library Kit (QIAGEN, Frederick, MD, USA). The quality of the library was verified using an Agilent 2100 Bioanalyzer (Agilent Technologies, USA). The samples, labeled with indices, were grouped using the cBot Cluster Generation System with the TruSeq PE Cluster Kit v3-cBot-HS (Illumina, San Diego, CA, USA) and then underwent high-throughput sequencing on the Illumina HiSeq platform (Echo Biotech Co., Ltd, China).[28]

The elimination and trimming process involved the removal of adaptor sequences, low-quality reads, contaminant reads, and reads that were either shorter than 18 nt or longer than 30 nt. The clean reads were aligned with various databases—Silva, Rfam, Repbase, and GtRNAdb—using Bowtie software. After filtering out ribosomal, transfer, small nuclear, and small nucleolar RNAs, the remaining reads were screened against miRbase and the mouse non-coding RNA sequence of Ensemble using miRDeep2. This screening aimed to identify known miRNAs and predict novel miRNAs. The read counts were normalized to the transcript copy number per million. Differentially expressed miRNAs among the groups were identified using the edgeR package. Statistical significance was defined as $p<0.05$ and a fold change ≥ 2.

Real-time RT-PCR

Total mRNA was extracted from HSCs and liver tissues using TRIzol reagent (Invitrogen, Carlsbad, CA), while QIAzol lysis reagent (Invitrogen, Carlsbad, CA) was used for miRNA extraction from HSCs and EVs. For mRNA quantification, reverse transcription was performed using High-Capacity cDNA Reverse Transcription Kits (Thermo Fisher Scientific, Rockford, IL, USA), and SYBR Green Master Mix (Invitrogen, Carlsbad, CA) was used to assess mRNA levels. For miRNA quantification, cDNA synthesis was carried out using the miScript II Reverse Transcription Kits (QIAGEN, Frederick, MD) and quantified using the miScript SYBR Green PCR Kit (QIAGEN, Frederick, MD). Real-time quantitative PCR was performed using a 7500 fast real-time PCR instrument (Applied Biosystems, Carlsbad, CA, USA). Each reaction was repeated at least five times, and the data were analyzed using the threshold cycle (Ct) method. mRNA normalization was performed against β-actin, and miRNA normalization was performed against the small RNA U6.[29,30] The sequences of primers used are listed in Supplementary Table 2.

Western blot

As described previously,[31] proteins were extracted from liver cells using a lysis buffer that included a protease/phosphatase inhibitor cocktail (KeyGEN BioTECH; Nanjing, China). The primary antibodies used were TIMP-1 (1:1,000, R & D), MCP-1 (1:2,000, Abcam, Cambridge, UK), Fli-1 (1:2,000, Abcam, Cambridge, UK), α-SMA (1:1,000, Sigma-Aldrich, St. Louis, MO, USA), collagen I (1:1,000, Abcam, Cambridge, UK), GAPDH (1:2,000, CST, Massachusetts, USA), and β-actin (1:5,000, Sigma-Aldrich, St. Louis, MO, USA). Subsequently, the membranes were incubated with the corresponding secondary antibodies for 2 h at room temperature (1:2,000, ZSGB-BIO, Beijing, China). The outcomes were observed through enhanced chemiluminescence assays (Thermo Fisher Scientific, Rockford, IL, USA).

Statistical analysis

The data is presented as the mean±SD. Statistical significance in two-group comparisons was assessed using the t-test. For comparisons involving three or more groups, a one-way analysis of variance was utilized. Statistical analyses were conducted using SPSS 25.0, Microsoft Excel, and GraphPad Prism 8.0. The threshold for statistical significance was established at $p<0.05$.

Results

Silencing TIMP-1 in CCl$_4$-induced mice alleviates liver fibrosis, macrophage recruitment, and MCP-1 expression

Histopathological changes in the liver were evaluated using

H&E and Masson staining in each experimental group. The CCl_4 and CCl_4+rAAV/EGFP groups exhibited severe fibrosis compared to the control group. The degree of liver fibrosis was significantly ameliorated after TIMP-1 silencing (Fig. 1A). Similar results were observed in the rat model (Supplementary Fig. 1A). The livers of mice and rats were immunostained with F4/80 or ED-1 to examine macrophage presence in the liver. Immunohistochemical analysis revealed heightened macrophage recruitment in the model and rAAV/EGFP groups, which was apparently reduced following rAAV/siRNA-TIMP-1 treatment (Fig. 1A, Supplementary Fig. 1A). Quantitative analysis showed a significant increase in the percentage of F4/80-positive cells in the model ($9.107\%\pm0.7566\%$) and rAAV/EGFP groups ($8.841\%\pm0.5735\%$) compared to the controls ($0.1920\%\pm0.0316\%$, $p<0.01$). Conversely, the rAAV/siRNA-TIMP-1 group exhibited a significant decrease ($5.459\%\pm0.1202\%$) compared to the model and rAAV/EGFP groups ($p<0.05$) (Fig. 1B), consistent with ED-1 staining results (Supplementary Fig. 1B).

RAAV/siRNA-TIMP-1 treatment reduced the expression of collagen I and α-SMA (Fig. 1C, F) compared to the model and rAAV/EGFP groups. Although there were no statistically significant differences in MMP13 gene expression between the rAAV/EGFP and rAAV/siRNA-TIMP-1 groups due to substantial variations within the groups, there was an observable trend of increased MMP13 expression in the rAAV/siRNA-TIMP-1 group compared to the rAAV/EGFP group (Fig. 1D). The expression of TIMP-1 and MCP-1 from the rAAV/siRNA-TIMP-1 group was decreased compared to the model and rAAV/EGFP groups in mice (Fig. 1E, F) and rats (Supplementary Fig. 1C–E). These findings collectively indicate that silencing TIMP-1 in mouse and rat fibrotic livers could improve the degree of fibrosis with decreased recruitment of hepatic macrophages and lower MCP-1 expression.

Downregulating TIMP-1 in mouse primary HSCs inhibits macrophage migration and suppresses MCP-1 expression

To investigate the direct impact of TIMP-1 silencing on macrophage recruitment, primary HSCs were employed using the transwell chamber assay. Immunofluorescence staining for desmin and α-SMA confirmed the high purity of the mouse primary HSCs, which were fully activated after five days of *in vitro* culture (Fig. 2A). Primary HSCs transfected with rAAV/EGFP enhanced RAW264.7 macrophage migration, whereas rAAV/siRNA-TIMP-1-transfected primary HSCs significantly diminished macrophage migration (Fig. 2B, C). Similar effects were observed in HSC-T6 and macrophage CRL-2192 (Supplementary Fig. 2A, B). To investigate whether TIMP-1 could influence MCP-1 expression, results showed that TIMP-1 deficiency apparently decreased the expression of MCP-1 protein and mRNA in primary HSCs (Fig. 2D, E) and HSC-T6 (Supplementary Fig. 2C–E). Collectively, these results demonstrate that TIMP-1 promotes macrophage migration by regulating MCP-1 expression *in vitro*.

TIMP-1 affects MCP-1 expression by inducing Fli-1 expression

Previous studies have shown that Fli-1 directly regulates MCP-1 expression. We speculate that TIMP-1 affects MCP-1 expression by regulating Fli-1 expression. We observed a notable reduction in Fli-1 mRNA (Fig. 3A) and protein (Fig. 3B) expression in the livers of mice treated with siRNA-TIMP-1, as opposed to the CCl_4 and rAAV/EGFP groups. This trend was consistent in the CCl_4-induced rat liver fibrosis model, where siRNA-TIMP-1 treatment resulted in a signifi-

cant decrease in Fli-1 expression (Supplementary Fig. 3A). Moreover, TIMP-1 knockdown in mouse primary HSCs (Fig. 3C, D) and HSC-T6 (Supplementary Fig. 3B, C) significantly downregulated both mRNA and protein levels of Fli-1. These results suggest that TIMP-1 affects Fli-1 expression both *in vivo* and *in vitro*.

Downregulation of Fli-1 expression in mouse primary HSCs by siRNA-Fli-1 transfection contributed to the decreased expression of MCP-1 mRNA and protein (Fig. 3E). Conversely, Fli-1 overexpression in mouse primary HSCs resulted in increased MCP-1 mRNA and protein levels (Fig. 3F), with consistent outcomes observed in HSC-T6 cells (Supplementary Fig. 3D). These results indicate that Fli-1 is a downstream regulator of TIMP-1, directly influencing MCP-1 expression.

TIMP-1 affects Fli-1 expression by regulating miRNA-145 expression

We explored the molecular mechanism by which TIMP-1 regulates Fli-1 expression. Predictive analysis was performed with microrna.org to investigate whether Fli-1 may be regulated by miRNAs. The website predictions identified miRNA-145 as a potential regulator of Fli-1 transcription. We speculate that TIMP-1 influences transcription factor Fli-1 expression through miRNA-145, thereby regulating MCP-1 expression.

As shown in Figure 4A, miRNA-145 expression was significantly increased in mouse primary HSCs (or HSC-T6, Supplementary Fig. 4A) after siRNA-TIMP-1 treatment. Transfection with miRNA-145 mimic (Fig. 4B, Supplementary Fig. 4B) resulted in decreased expression of both Fli-1 and MCP-1 in mouse primary HSCs (Fig. 4C, D) or HSC-T6 (Supplementary Fig. 4C). Conversely, the levels of Fli-1 and MCP-1 were significantly increased in mouse primary HSCs or HSC-T6 cells after transfection with miRNA-145 inhibitor (Fig. 4E, F, Supplementary Fig. 4D). Further, we examined whether miRNA-145 directly binds to the 3'-UTR of Fli-1 using luciferase reporter gene assays. These assays revealed two predicted binding sites for miRNA-145 in the 3'-UTR of Fli-1 (Fig. 4G). We constructed a series of luciferase reporter plasmids containing either the wild-type murine Fli-1 3'-UTR (WT) or the Fli-1 3'-UTR with single or combined mutations of miRNA-145 binding sites (Mut1, Mut2, or Mut1+2). Transfection of miRNA-145 mimic into 293 cells significantly reduced reporter activity, and single or combined mutations in the binding sites attenuated this effect (Fig. 4H). These findings collectively affirm that miRNA-145 directly targets the 3'-UTR of Fli-1.

EVs derived from TIMP-1 downregulated HSCs influence macrophage recruitment

EVs serve as mediators of intercellular communication, transferring bioinformation between cells and influencing cellular functions. The isolation of EVs from primary HSCs was confirmed by TEM analysis and the detection of specific markers (TSG101, CD9, and CD63) through western blotting (Fig. 5A). NTA further revealed a predominant size range of 50 to 150 nm for the EVs (Fig. 5B). Additionally, EVs labeled with PKH26 red fluorescent dye demonstrated their uptake by both HSCs and macrophages, underscoring their capacity to transmit information between these cell types (Fig. 5C). GW4869, a reversible inhibitor of neutral sphingomyelinase regulating EV secretion, was employed to examine whether EVs play a crucial role in TIMP-1-induced macrophage migration. The results of the transwell chamber assay revealed that the migration of macrophages co-cultured with HSCs transfected with siRNA-TIMP-1 or
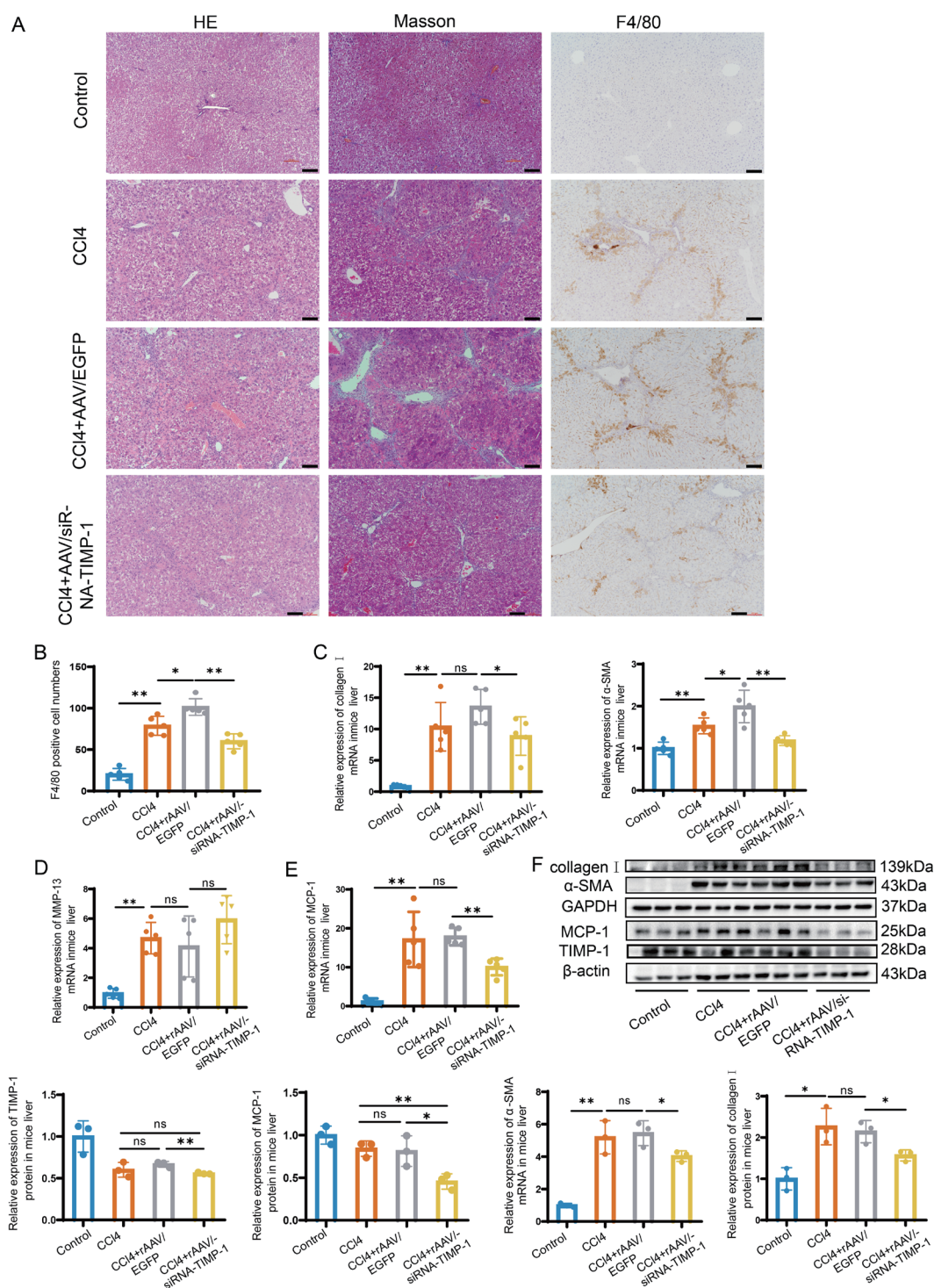
Fig. 1. Silencing of TIMP-1 in CCl₄-treated mice attenuates liver fibrosis and macrophage recruitment. Liver sections from control and CCl₄-treated mice administered the indicated therapeutic agent were stained for histological changes, collagen deposition, and macrophage migration by H&E, Masson, and F4/80 staining. (A) Representative H&E, Masson, and F4/80 staining of livers of control, CCl₄ and CCl₄ -treated mouse administered with rAAV/EGEP or rAAV/siRNA-TIMP-1. Scale bars: 100μm. (B) Percentage of F4/80 positive cells in 5 randomly selected microscopic fields. Scale bars: 100μm. (C)Transcript levels of collagen I and α-SMA in the livers of mice. (D) Transcript levels of MMP-13 in the livers of mice. (E) Transcript levels of MCP-1 in the livers of mice. (F) Immunoblot analysis of collagen I, α-SMA, TIMP-1, and MCP-1 in liver lysates of mice. β-actin and GAPDH content were detected as a loading control. * $p<0.05$, ** $p<0.01$, ns: not significant, versus the control group. Data are presented as mean±SD. TIMP-1, tissue inhibitor of metalloproteinase-1; CCl₄, carbon tetrachloride; H&E, hematoxylin and eosin; F4/80, EGF-like module-containing mucin-like hormone receptor-like 1; rAAV/EGFP, recombinant adeno-associated virus with enhanced green fluorescent protein; rAAV/siRNA-TIMP-1, recombinant adeno-associated virus with TIMP-1 gene-specific siRNA; collagen I, collagen type I; α-SMA, α-Smooth muscle actin; MMP-13, matrix metallopeptidase 13; MCP-1, monocyte chemoattractant protein-1; β-actin, Beta-actin; GAPDH, glyceraldehyde-3-phosphate dehydrogenase.
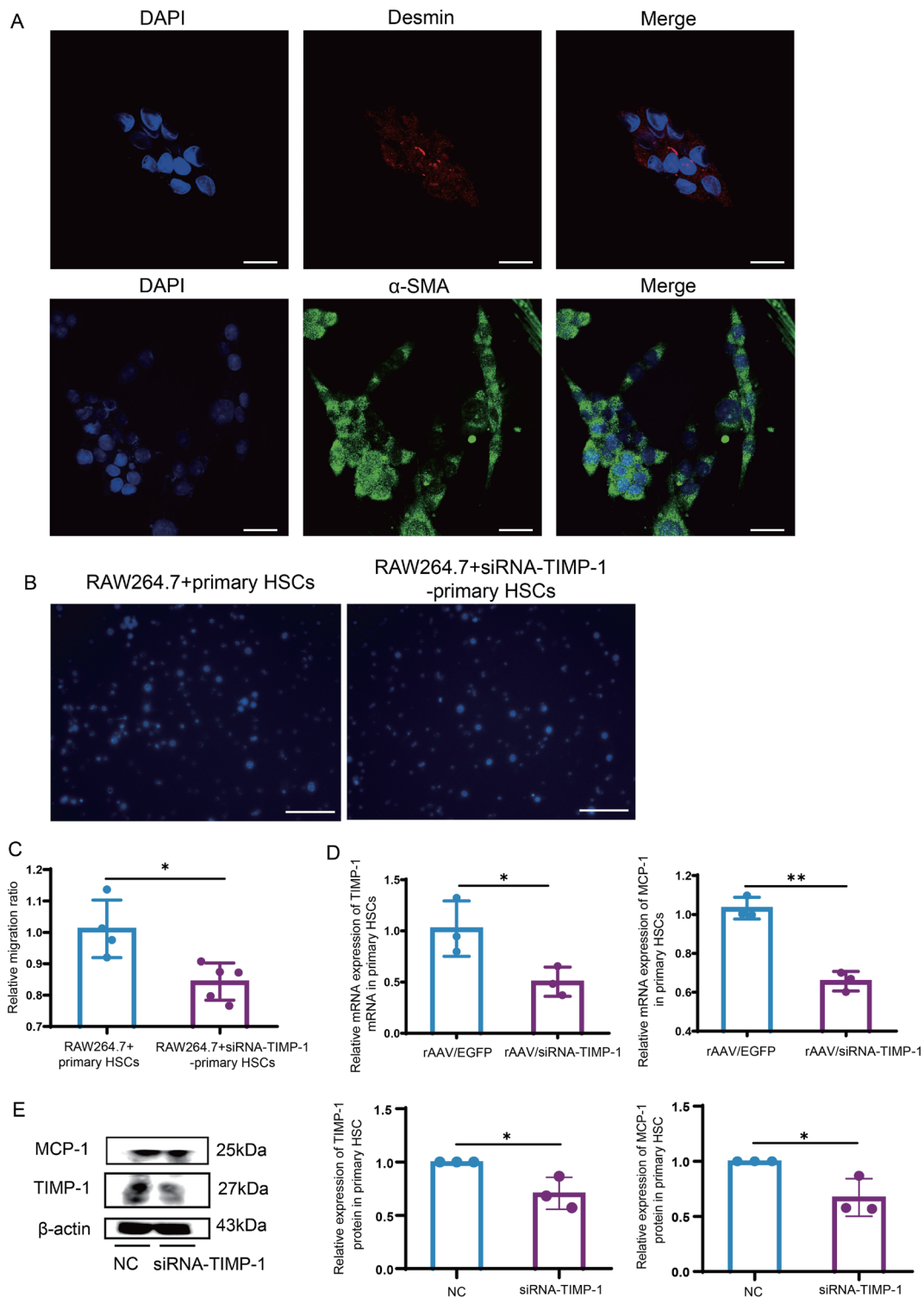
Fig. 2. Downregulation of TIMP-1 in primary HSCs from mice suppresses the macrophage migration and inhibits MCP-1 expression. (A) Desmin or α-SMA staining of isolated HSCs from mice. The cell nucleus was stained with DAPI. Scale bars: 20μm. (B) The migration ability of RAW264.7 cells was assessed by transwell migration assay. DAPI staining of representative lower surfaces of the chamber showed macrophage migration. Scale bars: 50μm. (C) Quantification of RAW264.7 cells migration. DAPI positive area of lower surfaces of the chamber was measured. (D) The transcript levels of TIMP-1 and MCP-1 in primary HSCs transfected with rAAV/siRNA-TIMP-1. (E) Immunoblot analysis of TIMP-1 and MCP-1 in primary HSCs transfected with rAAV/siRNA-TIMP-1. β-actin content was detected as a loading control. * $p<0.05$, ** $p<0.01$, versus the control group. Data are presented as mean±SD. TIMP-1, tissue inhibitor of metalloproteinase-1; HSCs, hepatic stellate cells; MCP-1, monocyte chemoattractant protein-1; β-actin, Beta-actin; α-SMA, α-Smooth muscle actin; DAPI, 4',6-diamidino-2-phenylindole; rAAV/siRNA-TIMP-1, recombinant adeno-associated virus with TIMP-1 gene-specific siRNA; NC, negative control.
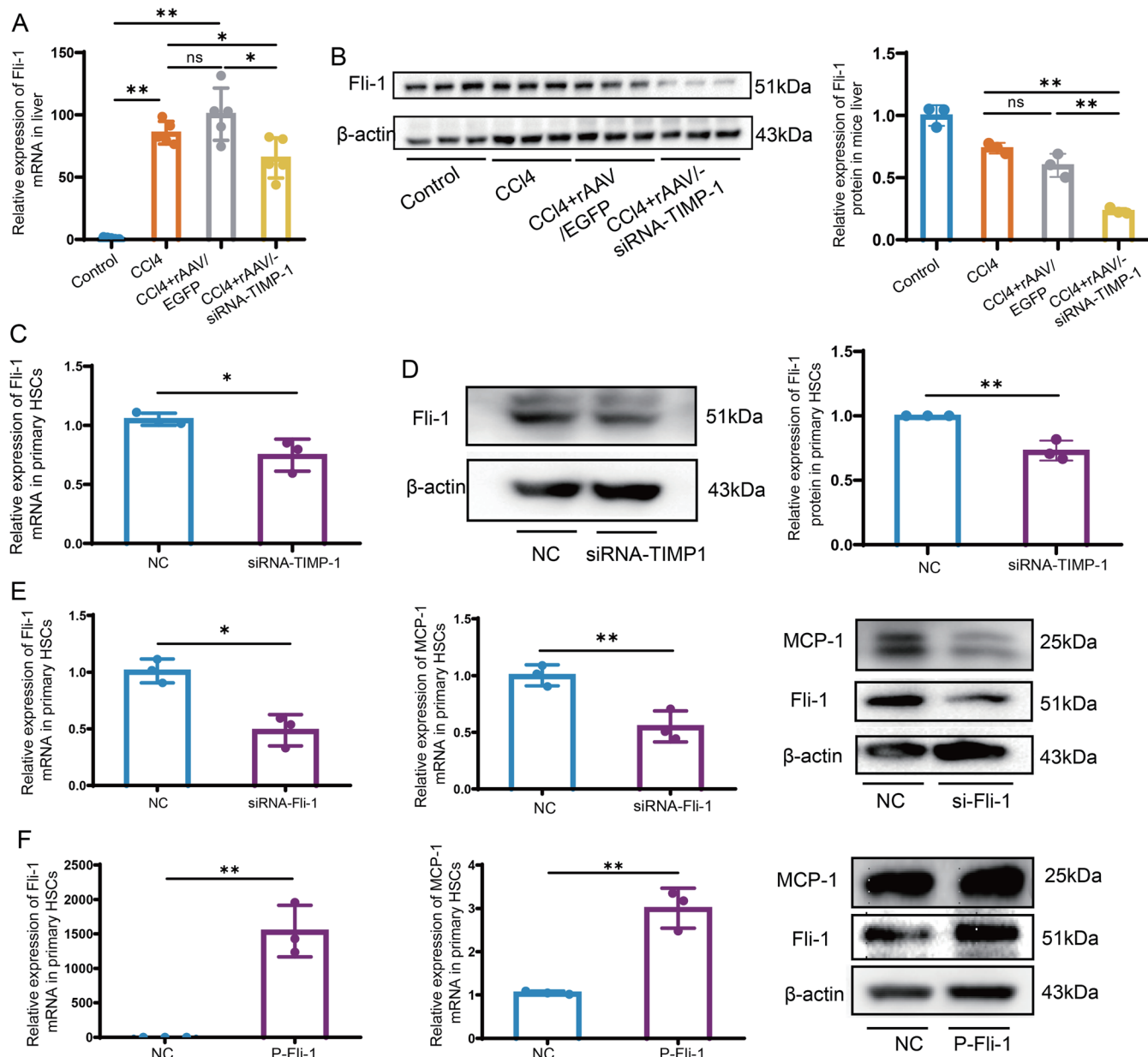
Fig. 3. TIMP-1 regulates the expression of MCP-1 via Fli-1 in mice and primary HSCs. (A) Transcript levels of Fli-1 in mice. (B) Immunoblot analysis of Fli-1 in liver lysates of mice. (C) The transcript levels of Fli-1 in primary HSCs transfected with siRNA-TIMP-1. (D) Immunoblot analysis of Fli-1 in primary HSCs transfected with siRNA-TIMP-1. (E) The transcript levels and immunoblot analysis of Fli-1 and MCP-1 in primary HSCs transfected with siRNA-Fli-1. (F) The transcript levels and immunoblot analysis of Fli-1 and MCP-1 in primary HSCs transfected with Fli-1 plasmid. * $p<0.05$, ** $p<0.01$, ns: not significant, versus the control group. Data are presented as mean±SD. TIMP-1, tissue inhibitor of metalloproteinase-1; CCl$_4$, carbon tetrachloride; rAAV/EGFP, recombinant adeno-associated virus with enhanced green fluorescent protein; rAAV/siRNA-TIMP-1, recombinant adeno-associated virus with TIMP-1 gene-specific siRNA; HSCs, hepatic stellate cells; MCP-1, monocyte chemoattractant protein-1; Fli-1, Friend leukemia integration 1; β-actin, Beta-actin; siRNA-TIMP-1, small interfering RNA targeting TIMP-1; siRNA-Fli-1, small interfering RNA targeting Fli-1; P-Fli-1, Fli-1 plasmid; NC, negative control.

NC by GW4869 pretreatment was not significantly different (Fig. 5D). These results illustrated that the decreased migration of macrophages mediated by HSCs after downregulation of TIMP-1 depended, at least in part, on the participation of EVs.

MiRNA-145 was enriched in EVs derived from HSCs after siRNA-TIMP-1 treatment

miRNA sequencing was performed to characterize the miRNA content of EVs and their parental cells. Forty-four miRNAs were found to be upregulated, and 76 miRNAs were downregulated in siRNA-TIMP-1 treated HSCs than controls. Moreover, 92 miRNAs were upregulated, and 128 miRNAs were downregulated in EVs derived from siRNA-TIMP-1-treated HSCs than controls. Among all the upregulated differential miRNAs both in HSCs and EVs, we chose the top 20 for our analysis, as shown in the heatmap (Fig. 6A). Subsequent predictive analyses using miRWalk.org, TargetScan.org, and
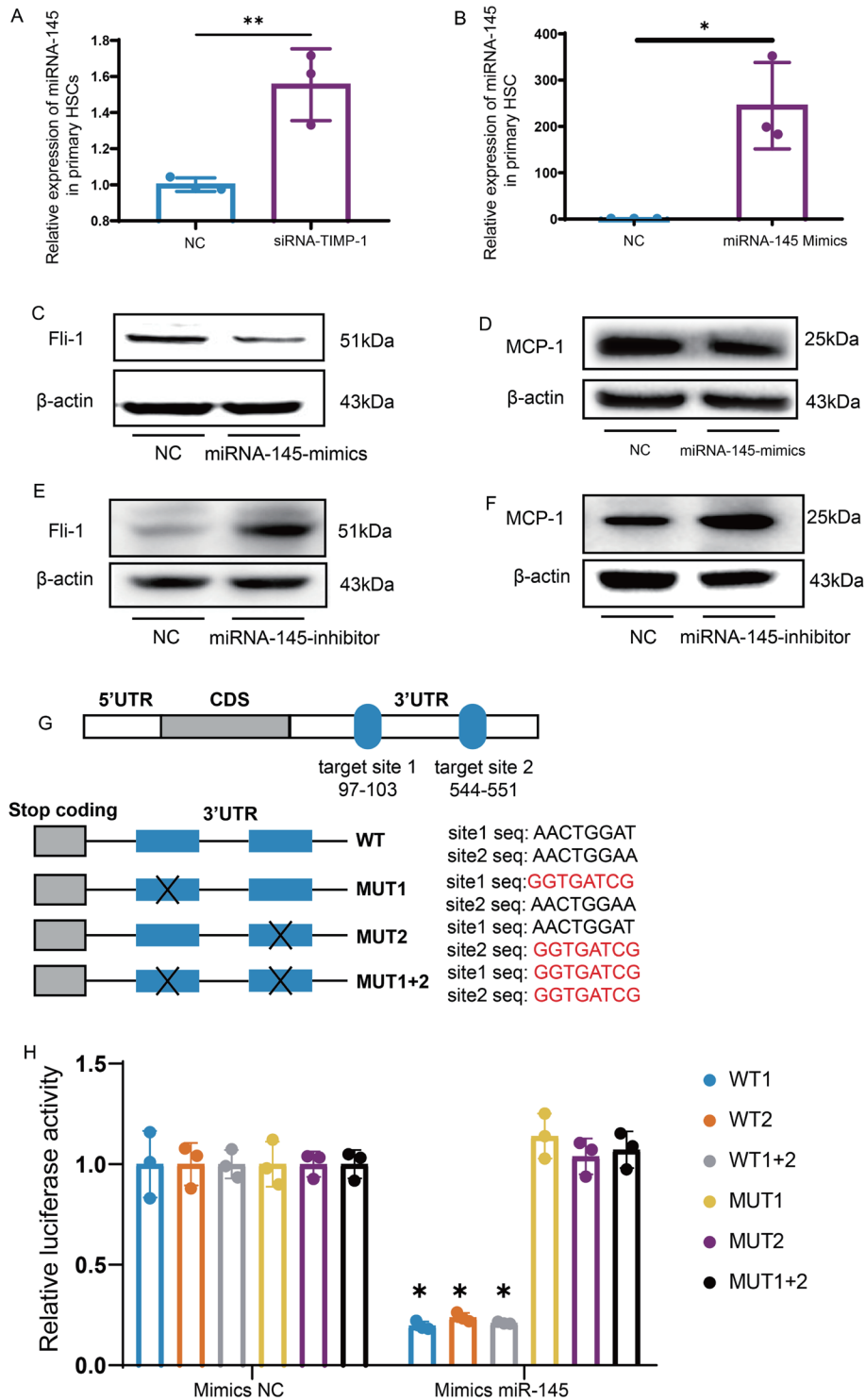
Fig. 4. TIMP-1 regulates the expression of Fli-1 through miRNA-145 in primary HSCs. (A) Transcript levels of miRNA-145 in primary HSCs transfected with siRNA-TIMP-1. (B) Transcript levels of miRNA-145 in primary HSCs transfected with miRNA-145 mimics. (C) Immunoblot analysis of Fli-1 in primary HSCs transfected with miRNA-145 mimics. (D) Immunoblot analysis of MCP-1 in primary HSCs transfected with miRNA-145 mimics. (E) Immunoblot analysis of Fli-1 in primary HSCs transfected with miRNA-145 inhibitor. (F) Immunoblot analysis of MCP-1 in primary HSCs transfected with miRNA-145 inhibitor. (G) Schematic structure of Fli-1 mRNA with two predicted miRNA-145 binding sites. Six different reporter vectors were constructed carrying the wild type or mutated Fli-1 3′untranslated region (UTR) mutation as indicated. (H) Relative luciferase activity of the indicated Fli-1 reporter constructs in 293 cells, co-transfected with miRNA-145 mimics or scramble mimics. * $p<0.05$, ** $p<0.01$, versus the control group. Data are presented as mean±SD. TIMP-1, tissue inhibitor of metalloproteinase-1; Fli-1, Friend leukemia integration 1; HSCs, hepatic stellate cells; MCP-1, monocyte chemoattractant protein-1; siRNA-TIMP-1, small interfering RNA targeting TIMP-1; miRNA-145, microRNA-145; WT, wild type; MUT, mutation; NC, negative control.
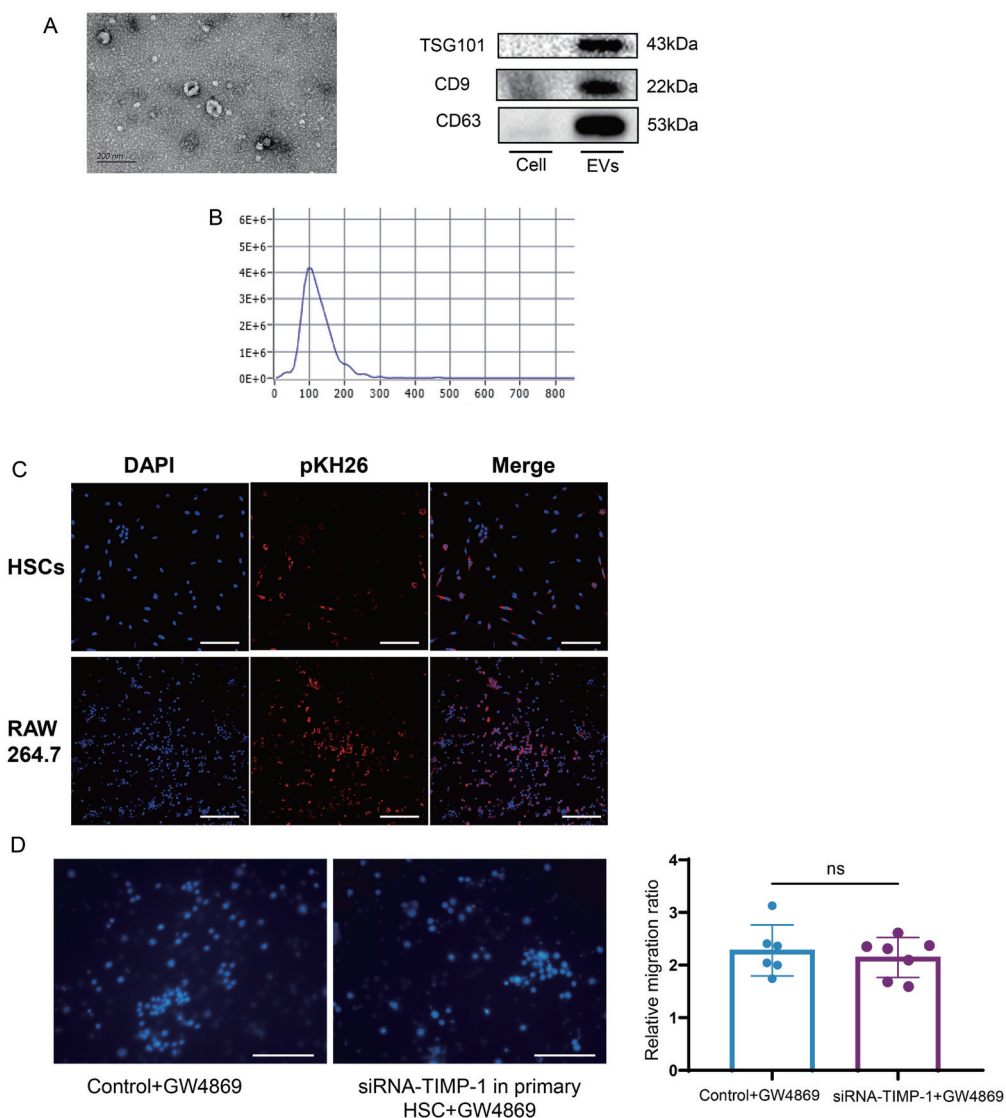
Fig. 5. EVs secreted by HSCs after TIMP-1 down-regulating can transfer information to surrounding HSCs and macrophages to influence macrophage recruitment. (A) TEM analysis of the purified EVs' integrity. Immunoblot analysis of mouse EVs specific markers TSG101, CD9, and CD63 in EVs. (B) NTA analysis of EVs' size. (C) Capture of HSC-derived EVs labeled with PKH26 (red fluorescence) by HSCs and macrophages (DAPI stained with blue fluorescence). Scale bars: 50μm. (D) The migration abilities of macrophages in both co-culture with HSCs that transfected with siRNA-TIMP-1 or NC by GW4869 pretreatment. Scale bars: 50μm. ns: not significant, versus the control group. Data are presented as mean±SD. EVs, extracellular vesicles; HSCs, hepatic stellate cells; TIMP-1, tissue inhibitor of metalloproteinase-1; TEM, transmission electron microscopy; TSG101, tumor susceptibility gene 101; CD9, cluster of differentiation-9; CD63, cluster of differentiation-63; NTA, analysis of nanoparticle tracking; siRNA-TIMP-1, small interfering RNA targeting TIMP-1; NC, negative control.

miRDB.org identified two miRNAs within the top 20 in EVs from siRNA-TIMP-1-treated HSCs, mmu-miRNA-145a-5p, and mmu-miR-92b-3p, that were predicted to bind to Fli-1 (Fig. 6B). Additionally, miRNA-145 showed the most significant difference between HSCs and EVs (Fig. 6C). We further verified the miRNA expression by real-time PCR and found that miRNA-145 in EVs was indeed elevated after inhibiting the expression of TIMP-1 in HSCs (Fig. 6D).

Discussion

TIMPs function as signaling molecules, exerting cytokine-like activities that impact cell growth, apoptosis, differentiation, angiogenesis, and oncogenesis.[11,32] TIMP-1, one of the four identified TIMPs, emerges as a significant player in toxic liver injury and cholestasis.[33–35] Several studies have documented that TIMP-1 not only hinders ECM degradation by suppressing MMP function but also inhibits the apoptosis of aHSCs, thereby promoting liver fibrosis.[7,36] Our study reveals a previously unidentified role of TIMP-1, demonstrating that it triggers the expression of Fli-1 via miRNA-145, which in turn raises MCP-1 levels and enhances macrophage recruitment.

Kupffer cells (liver-resident macrophages) and recruited macrophages can secrete fibrogenic cytokines that induce the transition of HSCs into ECM-producing myofibroblasts or further recruit inflammatory cells, contributing to liver fibrogenesis.[37,38] MCP-1, a crucial chemokine, promotes liver fibrosis by recruiting macrophages associated with HSC activation.[39,40] Additionally, MCP-1 contributes to macrophage infiltration in other diseases.[41] Our study revealed that MCP-
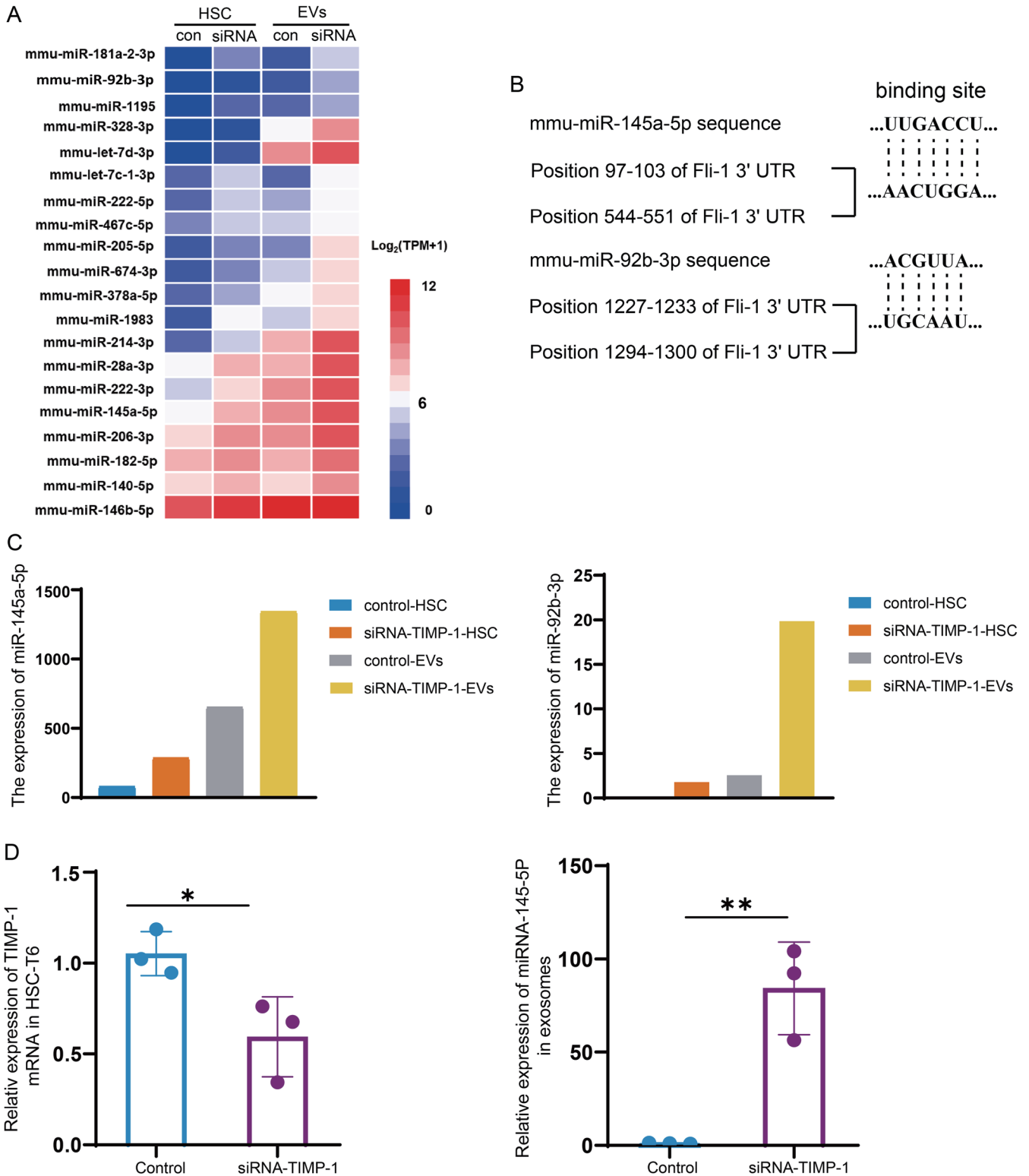
Fig. 6. Comparison of HSC- and EV-derived miRNAs' signatures between NC and siRNA-TIMP-1 treated HSCs. (A) The heatmap of top 20 upregulated differential miRNAs in HSCs and EVs. (B) The possible miRNA-145a-5p and miR-92b-3p binding sites were identified in the Fli-1 3'-UTR. (C) The expression of miRNA-145a-5p and miR-92b-3p in the results of RNA sequencing. (D) The transcript levels of TIMP-1 and miRNA-145 in HSCs and EVs after inhibiting the expression of TIMP-1 in HSCs. * $p < 0.05$, ** $p < 0.01$, versus the control group. Data are presented as mean±SD. EVs, extracellular vesicles, HSCs, hepatic stellate cells; NC, negative control; siRNA-TIMP-1, small interfering RNA targeting TIMP-1; Fli-1, Friend leukemia integration 1; TIMP-1, tissue inhibitor of metalloproteinase-1; miRNA-145, microRNA-145.

1 expression in liver tissue decreased after TIMP-1 downregulation in both rat and mouse models. An *in vitro* study also demonstrated that TIMP-1 deficiency decreased MCP-1 protein and mRNA expression in HSCs, along with suppressed macrophage migration. These data indicate that TIMP-1 mediates macrophage recruitment through MCP-1.

Reports indicated that the Fli-1 transcription factor directly regulates the expression of the chemokine MCP-1.[14] Our transient transfection assay further confirmed Fli-1's regulatory role in MCP-1 expression in HSCs. We then validated that the expression of Fli-1 mRNA and protein significantly decreased in HSCs after siRNA-TIMP-1 treatment. These results confirmed Fli-1 as a downstream regulator of TIMP-1, which regulates MCP-1 expression.

A growing body of evidence implicates different miRNAs in mediating TIMP-1's diverse functions.[12,42] In this study, we observed an increase in miRNA-145 expression after downregulating TIMP-1 in primary HSCs. Moreover, transfection with the miRNA-145 mimic resulted in decreased expression of Fli-1 and MCP-1, whereas transfection with the miRNA-145 inhibitor elicited the opposite effect. The dual luciferase reporter assay revealed the direct regulatory effect of miRNA-145 on Fli-1, which contains two binding sites for miRNA-145 in its 3'-UTR. To the best of our knowledge, this is the first observation of the TIMP-1/miRNA-145/Fli-1 interaction in HSCs. Combined with the evidence that Fli-1 can regulate MCP-1 expression, we conclude that the TIMP-1/miRNA-145/Fli-1 pathway in HSCs affects MCP-1 levels and macrophage recruitment.

MCP-1 can be produced not only by HSCs but also by Kupffer cells and liver sinusoidal endothelial cells, promoting the recruitment of macrophages to accelerate fibrosis.[43,44] Since TIMP-1 secreted by HSCs can regulate MCP-1 expression through miRNA-145, we assume that HSCs can transmit specific regulatory information, especially in the form of miRNAs, to surrounding HSCs or macrophages via EVs, thereby affecting macrophage recruitment. Initially, we verified that PKH26-labeled EVs from donor HSCs could be taken up by receptor HSCs and macrophages. Moreover, inhibiting EV secretion by HSCs reduced the migratory effect of TIMP-1 on macrophages. Increased miRNA-145 in EVs after lowering TIMP-1 suggests that these miRNA-rich EVs are crucial in HSC-macrophage communication and could be a new target for treating liver fibrosis. However, the function of other miRNAs enriched in EVs secreted from HSCs after TIMP-1 downregulation needs further study. Furthermore, it is necessary to elucidate whether miRNA-145 transferred from donor cells plays a crucial role in modulating MCP-1 expression in recipient cells.

The findings of this study highlight a novel regulatory mechanism wherein TIMP-1 influences macrophage recruitment in liver fibrosis by modulating MCP-1 through miRNA-145. This pathway presents a potential target for therapeutic intervention to mitigate macrophage-driven fibrogenesis. Targeting the TIMP-1/miRNA-145/MCP-1 axis clinically could result in innovative treatments disrupting macrophage recruitment and activation, potentially slowing or reversing liver fibrosis progression. Furthermore, the role of miRNA-145-enriched extracellular vesicles in mediating intercellular communication offers a novel avenue for therapeutic strategies that could harness or mimic these natural processes to modulate fibrotic pathways. Focusing on these molecular interactions might lead to more targeted future therapies, reducing side effects and improving efficacy for patients with chronic liver diseases.

Conclusion

In summary, TIMP-1 induces the expression of the transcrip-

tion factor Fli-1 through miRNA-145, consequently elevating MCP-1 expression. MiRNA-145-enriched EVs released from HSCs can transmit biological information to surrounding HSCs and macrophages and magnify the function of TIMP-1. The expression of TIMP-1 in HSCs exacerbates the progression of hepatic fibrosis by fostering macrophage recruitment.

Funding

Conflict of interest

JJ has been an Executive Associate Editor of *Journal of Clinical and Translational Hepatology* since 2013. The other authors have no conflict of interests related to this publication.

Author contributions

Material preparation, data collection and drafting of the manuscript (XH, XW, YW), data analysis (SS, WC), technical support (TL, PW, XF, LL), study supervision (JJ), and study concept, design, and supervision (MC). All authors have made significant contributions to this study and have approved the final manuscript.

Ethical statement

All animal care and experimental procedures complied with the guidelines for the use of laboratory animals drawn up by the Beijing Friendship Hospital, Capital Medical University (approval number: 18-2001, Beijing, China). All animals received humane care.

Data sharing statement

All data are available upon request.

References

[1] Asrani SK, Devarbhavi H, Eaton J, Kamath PS. Burden of liver diseases in the world. J Hepatol 2019;70(1):151–171. doi:10.1016/j.jhep.2018.09.014, PMID:30266282.
[2] Younossi ZM, Wong G, Anstee QM, Henry L. The Global Burden of Liver Disease. Clin Gastroenterol Hepatol 2023;21(8):1978–1991. doi:10.1016/j.cgh.2023.04.015, PMID:37121527.
[3] Kisseleva T, Brenner D. Molecular and cellular mechanisms of liver fibrosis and its regression. Nat Rev Gastroenterol Hepatol 2021;18(3):151–166. doi:10.1038/s41575-020-00372-7, PMID:33128017.
[4] Friedman SL, Pinzani M. Hepatic fibrosis 2022: Unmet needs and a blueprint for the future. Hepatology 2022;75(2):473–488. doi:10.1002/hep.32285, PMID:34923653.
[5] Molière S, Jaulin A, Tomasetto CL, Dali-Youcef N. Roles of Matrix Metalloproteinases and Their Natural Inhibitors in Metabolism: Insights into Health and Disease. Int J Mol Sci 2023;24(13):10649. doi:10.3390/ijms241310649, PMID:37445827.
[6] Cai X, Wang J, Wang J, Zhou Q, Yang B, He Q, *et al*. Intercellular crosstalk of hepatic stellate cells in liver fibrosis: New insights into therapy. Pharmacol Res 2020;155:104720. doi:10.1016/j.phrs.2020.104720, PMID:32092405.
[7] Murphy FR, Issa R, Zhou X, Ratnarajah S, Nagase H, Arthur MJ, *et al*. Inhibition of apoptosis of activated hepatic stellate cells by tissue inhibitor of metalloproteinase-1 is mediated via effects on matrix metalloproteinase inhibition: implications for reversibility of liver fibrosis. J Biol Chem 2002;277(13):11069–11076. doi:10.1074/jbc.M111490200, PMID:11796725.
[8] Ries C. Cytokine functions of TIMP-1. Cell Mol Life Sci 2014;71(4):659–672. doi:10.1007/s00018-013-1457-3, PMID:23982756.
[9] Cong M, Liu T, Wang P, Fan X, Yang A, Bai Y, *et al*. Antifibrotic effects of a recombinant adeno-associated virus carrying small interfering RNA targeting TIMP-1 in rat liver fibrosis. Am J Pathol 2013;182(5):1607–1616. doi:10.1016/j.ajpath.2013.01.036, PMID:23474083.
[10] Li M, Chen L, Gao Y, Li M, Wang X, Qiang L, *et al*. Recent advances tar-

geting C-C chemokine receptor type 2 for liver diseases in monocyte/macrophage. Liver Int 2020;40(12):2928–2936. doi:10.1111/liv.14687, PMID:33025657.

[11] Ghoshal-Gupta S, Kutiyanawalla A, Lee BR, Ojha J, Nurani A, Mondal AK, *et al*. TIMP-1 downregulation modulates miR-125a-5p expression and triggers the apoptotic pathway. Oncotarget 2018;9(10):8941–8956. doi:10.18632/oncotarget.23832, PMID:29507665.

[12] Cui H, Seubert B, Stahl E, Dietz H, Reuning U, Moreno-Leon L, *et al*. Tissue inhibitor of metalloproteinases-1 induces a pro-tumourigenic increase of miR-210 in lung adenocarcinoma cells and their exosomes. Oncogene 2015;34(28):3640–3650. doi:10.1038/onc.2014.300, PMID:25263437.

[13] Zhang J, Guo H, Zhang H, Wang H, Qian G, Fan X, *et al*. Putative tumor suppressor miR-145 inhibits colon cancer cell growth by targeting oncogene Friend leukemia virus integration 1 gene. Cancer 2011;117(1):86–95. doi:10.1002/cncr.25522, PMID:20737575.

[14] Lennard Richard ML, Nowling TK, Brandon D, Watson DK, Zhang XK. Fli-1 controls transcription from the MCP-1 gene promoter, which may provide a novel mechanism for chemokine and cytokine activation. Mol Immunol 2015;63(2):566–573. doi:10.1016/j.molimm.2014.07.013, PMID:25108845.

[15] Wu P, Liang J, Yu F, Zhou Z, Tang J, Li K. miR-145 promotes osteosarcoma growth by reducing expression of the transcription factor friend leukemia virus integration 1. Oncotarget 2016;7(27):42241–42251. doi:10.18632/oncotarget.9948, PMID:27304058.

[16] Chen L, Brenner DA, Kisseleva T. Combatting Fibrosis: Exosome-Based Therapies in the Regression of Liver Fibrosis. Hepatol Commun 2019;3(2):180–192. doi:10.1002/hep4.1290, PMID:30766956.

[17] Hu X, Ge Q, Zhang Y, Li B, Cheng E, Wang Y, *et al*. A review of the effect of exosomes from different cells on liver fibrosis. Biomed Pharmacother 2023;161:114415. doi:10.1016/j.biopha.2023.114415, PMID:36812711.

[18] Liu X, Xu J, Rosenthal S, Zhang LJ, McCubbin R, Meshgin N, *et al*. Identification of Lineage-Specific Transcription Factors That Prevent Activation of Hepatic Stellate Cells and Promote Fibrosis Resolution. Gastroenterology 2020;158(6):1728–1744.e14. doi:10.1053/j.gastro.2020.01.027, PMID:31982409.

[19] Xiu AY, Ding Q, Li Z, Zhang CQ. Doxazosin Attenuates Liver Fibrosis by Inhibiting Autophagy in Hepatic Stellate Cells via Activation of the PI3K/Akt/mTOR Signaling Pathway. Drug Des Devel Ther 2021;15:3643–3659. doi:10.2147/DDDT.S317701, PMID:34456560.

[20] Aoyama T, Inokuchi S, Brenner DA, Seki E. CX3CL1-CX3CR1 interaction prevents carbon tetrachloride-induced liver inflammation and fibrosis in mice. Hepatology 2010;52(4):1390–1400. doi:10.1002/hep.23795, PMID:20683935.

[21] Siegmund SV, Uchinami H, Osawa Y, Brenner DA, Schwabe RF. Anandamide induces necrosis in primary hepatic stellate cells. Hepatology 2005;41(5):1085–1095. doi:10.1002/hep.20667, PMID:15841466.

[22] Gao H, Jin Z, Bandyopadhyay G, Wang G, Zhang D, Rocha KCE, *et al*. Aberrant iron distribution via hepatocyte-stellate cell axis drives liver lipogenesis and fibrosis. Cell Metab 2022;34(8):1201–1213.e5. doi:10.1016/j.cmet.2022.07.006, PMID:35921818.

[23] Mejias M, Gallego J, Naranjo-Suarez S, Ramirez M, Pell N, Manzano A, *et al*. CPEB4 Increases Expression of PFKFB3 to Induce Glycolysis and Activate Mouse and Human Hepatic Stellate Cells, Promoting Liver Fibrosis. Gastroenterology 2020;159(1):273–288. doi:10.1053/j.gastro.2020.03.008, PMID:32169429.

[24] Du J, Wan Z, Wang C, Lu F, Wei M, Wang D, *et al*. Designer exosomes for targeted and efficient ferroptosis induction in cancer via chemo-photodynamic therapy. Theranostics 2021;11(17):8185–8196. doi:10.7150/thno.59121, PMID:34373736.

[25] Jiang R, Luo S, Zhang M, Wang W, Zhuo S, Wu Y, *et al*. Ginsenoside Rh4 inhibits inflammation-related hepatocellular carcinoma progression by targeting HDAC4/IL-6/STAT3 signaling. Mol Genet Genomics 2023;298(6):1479–1492. doi:10.1007/s00438-023-02070-w, PMID:37843550.

[26] Chen Y, Sun J, Liu J, Wei Y, Wang X, Fang H, *et al*. Aldehyde dehydrogenase 2-mediated aldehyde metabolism promotes tumor immune evasion by regulating the NOD/VISTA axis. J Immunother Cancer 2023;11(12):e007487. doi:10.1136/jitc-2023-007487, PMID:38088186.

[27] Chen L, Chen R, Kemper S, Cong M, You H, Brigstock DR. Therapeutic effects of serum extracellular vesicles in liver fibrosis. J Extracell Vesicles 2018;7(1):1461505. doi:10.1080/20013078.2018.1461505, PMID:29696080.

[28] Zhou Q, Rong C, Gu T, Li H, Wu L, Zhuansun X, *et al*. Mesenchymal stem cells improve liver fibrosis and protect hepatocytes by promoting microRNA-148a-5p-mediated inhibition of Notch signaling pathway. Stem Cell Res Ther 2022;13(1):354. doi:10.1186/s13287-022-03030-8, PMID:35883205.

[29] Zhang Y, Tan YY, Chen PP, Xu H, Xie SJ, Xu SJ, *et al*. Genome-wide identification of microRNA targets reveals positive regulation of the Hippo pathway by miR-122 during liver development. Cell Death Dis 2021;12(12):1161. doi:10.1038/s41419-021-04436-7, PMID:34907157.

[30] Li Y, Ouyang Q, Chen W, Liu K, Zhang B, Yao J, *et al*. An iron-dependent form of non-canonical ferroptosis induced by labile iron. Sci China Life Sci 2023;66(3):516–527. doi:10.1007/s11427-022-2244-4, PMID:36515861.

[31] Li Y, Ouyang Q, Chen Z, Chen W, Zhang B, Zhang S, *et al*. Intracellular labile iron is a key regulator of hepcidin expression and iron metabolism. Hepatol Int 2023;17(3):636–647. doi:10.1007/s12072-022-10452-2, PMID:36512269.

[32] Dolmatov IY, Nizhnichenko VA, Dolmatova LS. Matrix Metalloproteinases and Tissue Inhibitors of Metalloproteinases in Echinoderms: Structure and Possible Functions. Cells 2021;10(9):2331. doi:10.3390/cells10092331, PMID:34571980.

[33] Shan L, Wang F, Zhai D, Meng X, Liu J, Lv X. Matrix metalloproteinases induce extracellular matrix degradation through various pathways to alleviate hepatic fibrosis. Biomed Pharmacother 2023;161:114472. doi:10.1016/j.biopha.2023.114472, PMID:37002573.

[34] Gieling RG, Burt AD, Mann DA. Fibrosis and cirrhosis reversibility - molecular mechanisms. Clin Liver Dis 2008;12(4):915–937. doi:10.1016/j.cld.2008.07.001, PMID:18984474.

[35] Arendt E, Ueberham U, Bittner R, Gebhardt R, Ueberham E. Enhanced matrix degradation after withdrawal of TGF-beta1 triggers hepatocytes from apoptosis to proliferation and regeneration. Cell Prolif 2005;38(5):287–299. doi:10.1111/j.1365-2184.2005.00350.x, PMID:16202037.

[36] Yoshiji H, Kuriyama S, Yoshii J, Ikenaka Y, Noguchi R, Nakatani T, *et al*. Tissue inhibitor of metalloproteinases-1 attenuates spontaneous liver fibrosis resolution in the transgenic mouse. Hepatology 2002;;36(4 Pt 1):850–860. doi:10.1053/jhep.2002.35625, PMID:12297832.

[37] Schuppan D, Ashfaq-Khan M, Yang AT, Kim YO. Liver fibrosis: Direct antifibrotic agents and targeted therapies. Matrix Biol 2018;68-69:435–451. doi:10.1016/j.matbio.2018.04.006, PMID:29656147.

[38] Sun M, Kisseleva T. Reversibility of liver fibrosis. Clin Res Hepatol Gastroenterol 2015;39 Suppl 1:S60–S63. doi:10.1016/j.clinre.2015.06.015, PMID:26206574.

[39] Filliol A, Schwabe RF. FoxM1 Induces CCl2 Secretion From Hepatocytes Triggering Hepatic Inflammation, Injury, Fibrosis, and Liver Cancer. Cell Mol Gastroenterol Hepatol 2020;9(3):555–556. doi:10.1016/j.jcmgh.2020.01.002, PMID:32008983.

[40] Flamini S, Sergeev P, Viana de Barros Z, Mello T, Biagioli M, Paglialunga M, *et al*. Glucocorticoid-induced leucine zipper regulates liver fibrosis by suppressing CCL2-mediated leukocyte recruitment. Cell Death Dis 2021;12(5):421. doi:10.1038/s41419-021-03704-w, PMID:33927191.

[41] Singh S, Anshita D, Ravichandiran V. MCP-1: Function, regulation, and involvement in disease. Int Immunopharmacol 2021;101(Pt B):107598. doi:10.1016/j.intimp.2021.107598, PMID:34233864.

[42] Egea V, Zahler S, Rieth N, Neth P, Popp T, Kehe K, *et al*. Tissue inhibitor of metalloproteinase-1 (TIMP-1) regulates mesenchymal stem cells through let-7f microRNA and Wnt/β-catenin signaling. Proc Natl Acad Sci U S A 2012;109(6):E309–E316. doi:10.1073/pnas.1115083109, PMID:22223664.

[43] She S, Ren L, Chen P, Wang M, Chen D, Wang Y, *et al*. Functional Roles of Chemokine Receptor CCR2 and Its Ligands in Liver Disease. Front Immunol 2022;13:812431. doi:10.3389/fimmu.2022.812431, PMID:35281057.

[44] Gao J, Wei B, Liu M, Hirsova P, Sehrawat TS, Cao S, *et al*. Endothelial p300 Promotes Portal Hypertension and Hepatic Fibrosis Through C-C Motif Chemokine Ligand 2-Mediated Angiocrine Signaling. Hepatology 2021;73(6):2468–2483. doi:10.1002/hep.31617, PMID:33159815.